Mykhailo Orlyuk, Andrii Romenets, Andrii Marchenko

Subbotin Institute of Geophysics of the National Academy of Sciences of Ukraine, Kyiv
E-mail: orliuk@ukr.net, andrey_marchenko@ukr.net, romenets@ukr.net

GEOMAGNETIC OBSERVATIONS IN THE VICINITY OF THE "STRUVE GEODETIC ARC" DURING STRONG MAGNETIC STORMS: INITIAL DATA AND THEIR PRELIMINARY INTERPRETATION

VIRAC Scientific Seminar, IONIX Project, 26 Feb 2026

This research was funded by Latvian Council of Science, Fundamental and Applied Research Project “Characterisation of Extreme Space Weather Effects in the Ionosphere (IONEX)”, grant number lzp-2025/1-0067”

Earth's magnetic field

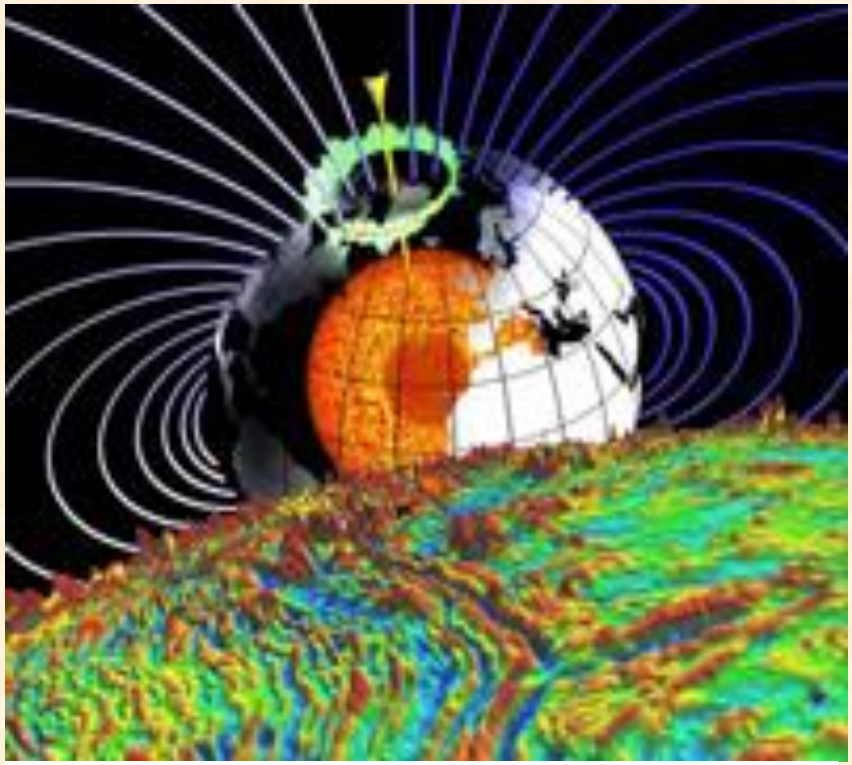

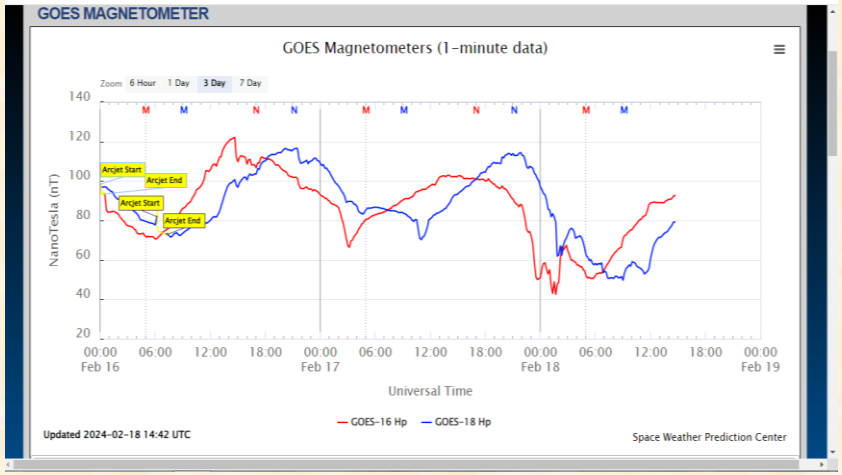

Earth's magnetic field (EMF) is determined by the sum of fields from different sources:

$$B = Bc + Bl + Be$$

where B is the EMF induction module, Bc is the main (core) EMF (B_{IGRF}), Bl is the lithospheric magnetic field, and Be is the external magnetic field. The main field is caused by mechanical and electromagnetic processes in the outer layer of the Earth's core; the field of the lithosphere is related to the magnetization of its rocks; the external field is caused by electric currents that exist in near-Earth space and are induced in the Earth's lithosphere and mantle.

Introduction

One of the main components of the solar-terrestrial interactions is the magnetic field. It, on the one hand, serves as a link between the Sun and the Earth, and, on the other hand, causes a different response to the same impact depending on the "relief" of the Earth's internal magnetic field. In this regard, the work (Orlyuk et al., 2025) investigated the nature of the magnetic storm on May 24, 2024 in the vicinity of the Struve Geodetic Arc (SGA) meridian. The results were presented at the 9th International Scientific Conference "Baltic Applied Astroinformatics and Space Data Processing", November 12th – 13th, 2025. The SGA meridian is characterized by significant changes in the Earth's main magnetic field (core field) and anomalous magnetic field (lithosphere field).

To determine the relationship between the geomagnetic field and geomagnetic disturbances caused by solar activity on 10.05.2024–13.05.2024, **we used the DGRF/IGRF model of the Earth's main magnetic field** [Brown et.al, 2021; International..., 2021], **digital maps of the anomalous magnetic field *ΔB*** [Korhonen, et al. 2007; Meyer et.al. 2017;Liu et.all., 2023], **the model of the geomagnetic field induction module *B*** [Enhansed..., 2017] **and data of variations of the module *B* and its components *Bx, By, Bz* from 7 magnetic observatories** [https://intermagnet.org/] **in the area of the SGA meridian**.

The above publication and report presented the results of a study of the internal and external geomagnetic field perturbations along the Struve arc based on the analysis of its variations in 7 magnetic observatories. The main results of this study are as follows:

Research in the area of the Struve arc makes it possible to detect the solar-terrestrial “magnetic” connection at both the planetary and regional levels.

- The normal magnetic field BIGRF changes regularly from south to north. This should lead to a corresponding change in the variations of the geomagnetic field.

- The increase in the BIGRF field induction modulus for the northern part of the SGA by 830÷930 nT (for the time interval 10-13.05.2024 - 29-31. 2003) caused a stronger manifestation of the magnetic storm and a shift of its maximum disturbances by 4 degrees to the south.

- The potentional connection of the geomagnetic storm maximum manifestation with the Earth's surface regional magnetic anomalies and their superpositional manifestation at an altitude of 100 km was revealed.

- The influence of the latter on the formation of ionospheric currents can be considered the most likely mechanism of connection between the amplitude of the external field variations and the Earth's main and lithospheric magnetic fields module.

The Struve Geodetic Arc: internal magnetic field of the Earth

The arc was measured from 1816 to 1855 at the distance from Fuglenes (in the vicinity of Hammerfest near Cape Nordkapp, Norway, 70° 40' 12" N, 23° 39' 48" E) to Staro-Nekrasivka in the vicinity of Izmail (Odesa Region, 45° 19 ' 54" N, 28° 55' 41" E). It is a meridian arc with a length of 2821.833 km and an amplitude of 25° 20′ 08″.

Currently, the issues of solar-terrestrial connections are very relevant, especially the mechanisms of transmission of deep space disturbances to the Earth's surface. (*Cnossen, I., A.D. Richmond, and M. Wiltberger, The dependence of the coupled magnetosphere-ionosphere-thermosphere system on the Earth's magnetic dipole moment (2012). J. Geophys. Res., 117, A05302, DOI:10.1029/2012JA017555; Orlyuk M.I., Romenets A.A. Spatial-temporal change of the geomagnetic field: environmental aspect//Геофизич. Журнал. — 2020. — т.42, № 4. — С.18 -38. DOI: https://doi.org/10.24028/gzh.0203-3100.v42i4.2020.210670*]).

Main magnetic field B_{IGRF} in the "Struve Arc" region for the Epoch 2024,5

On the nearsurface (4 km) of the Earth

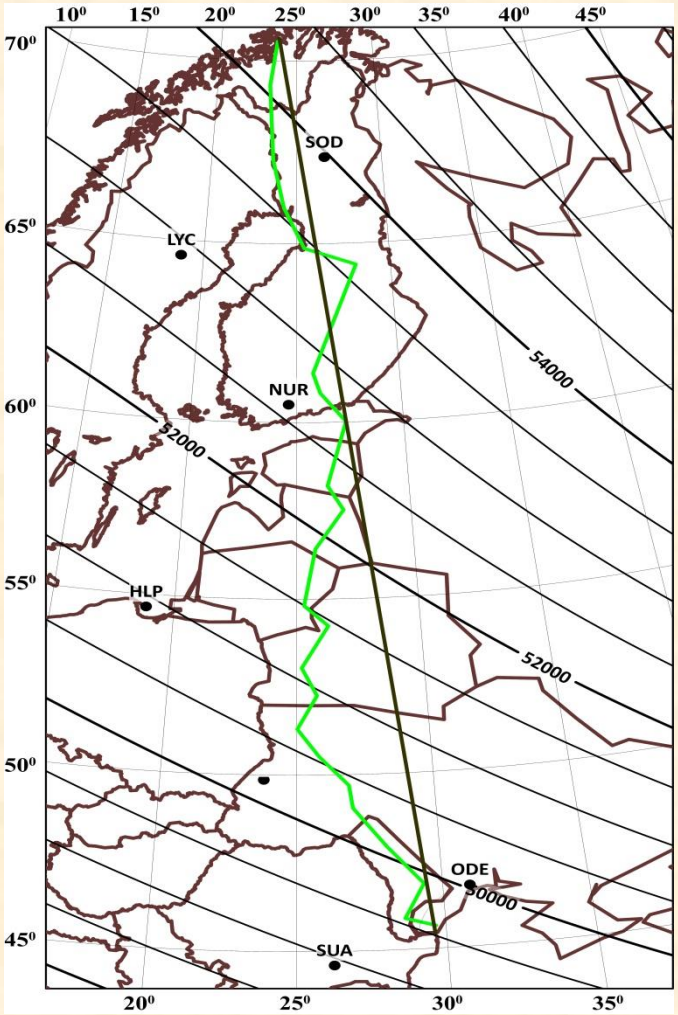

At an altitude of 100 km

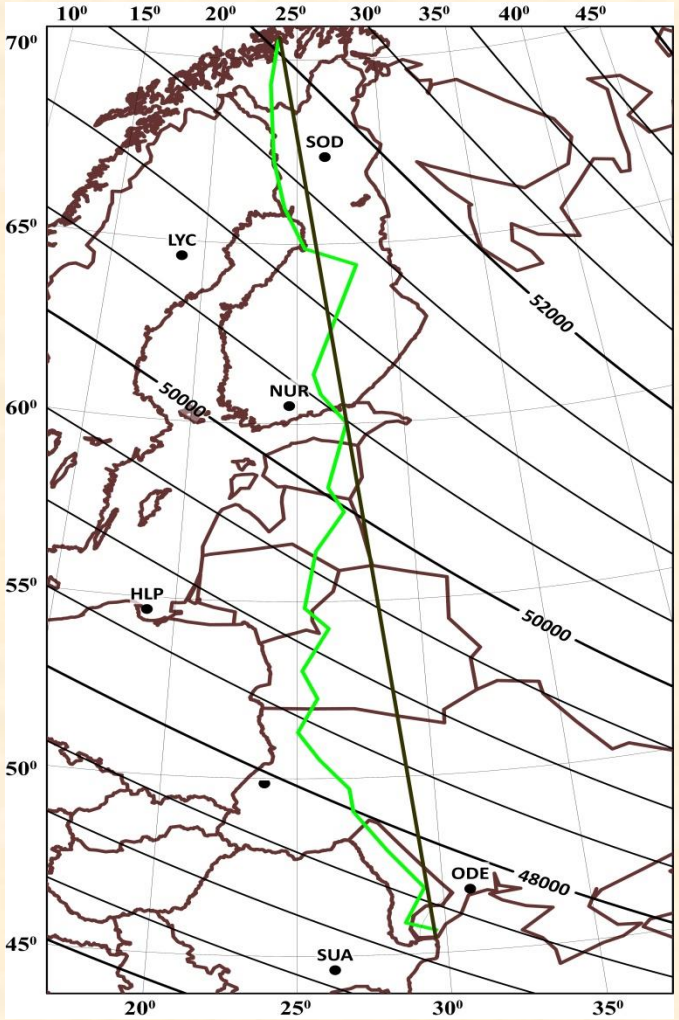

Observatories:

Sodankyla (SOD)
(67.37N, 26.63E)
Lycksele (LYC)
(64.612N, 18.748E)
Nurmijarvi (NUR)
(60.51N, 24.66E)
Hel (HLP)
(54.6035N, 18.8107E)
Lviv (LVV)
(49.90N, 23.75E)
Odesa (ODE)
(46.783N, 30.883E)
Surlari (SUR)
(44.68N, 26.25E

The normal magnetic field BIGRF changes regularly from south to north: (49,500 – 54,500) nT on the nearsurface (4 km) of the Earth ; (47,000 – 52,000) - at an altitude of 100 km.

The induction modulus of the B_{IGRF} field varies from 49,500 nT in the south of the territory to 54,500 nT in the north. The inclination and declination of the vector change from I=62.8°, D=6.9° in the south of the territory to I=78.8°, **D=13.8° in its north on the Earth's surface.**

At an altitude of 100 km, the B_{IGRF} field modulus varies from 47,000 nT in the south of the territory to 52,000 nT in its north. The inclination and declination of the vector change from I = 62.6°, D = 6.7° in the south of **the territory to I = 78.8°, D = 13.1° in its north**

In addition to the Intermagnet observatories [https://intermagnet.org/] we are using the data of the IMAGE programme: https://space.fmi.fi/image/www/index.php?page=rules_of_road /. We are sincerely grateful to the staff of these observatories for the opportunity to use digital data of 1-second and 1-minute observations. Special thanks to the Institute of Geophysics of the Polish Academy of Sciences, who provided data from two magnetic stations (Birzai and Suwałki), located near Ventspils.

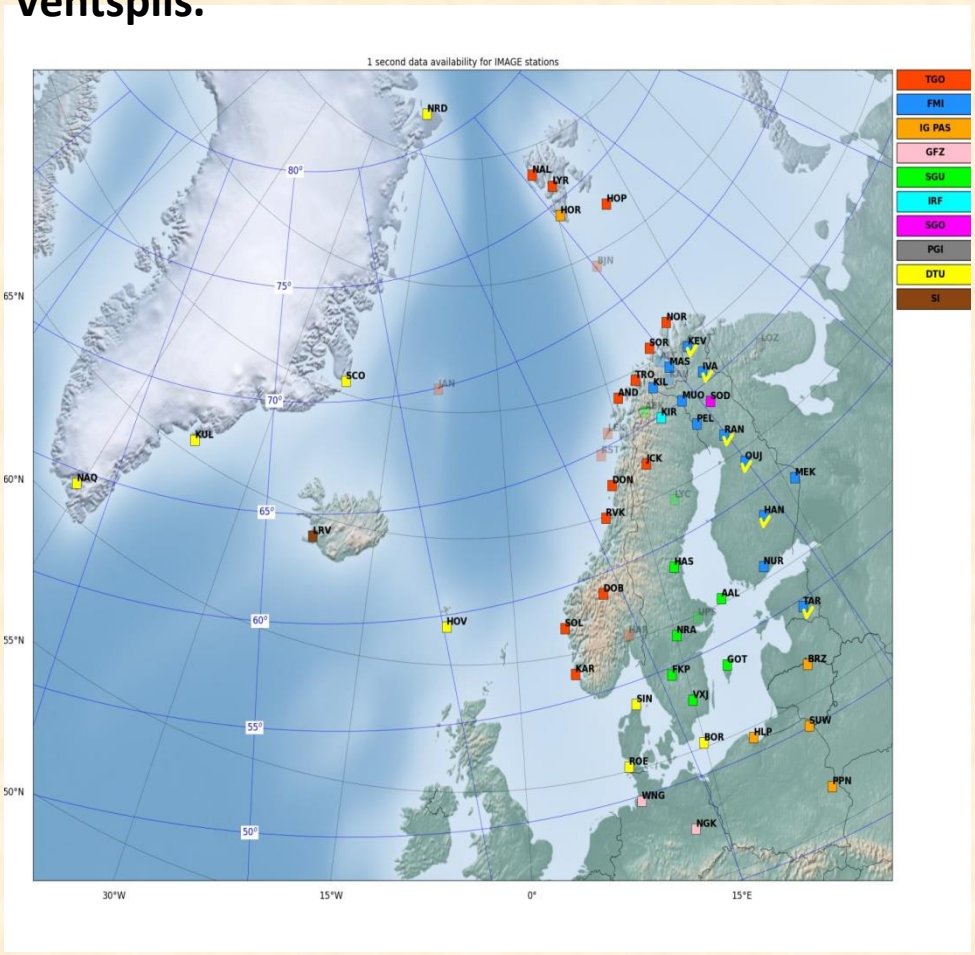

As part of the IONEX project, we processed data for two strong magnetic storms on November 11-14, 2025 and January 18-22, 2026 for 17 observatories and magnetic stations

Kod	Name (country)	Latitude	Longitude
KEV	Kevo (Finland)	69,76	27,01
IVA	Ivalo (Finland)	68,56	27,29
SOD	Sodankylä (Finland)	67,37	26,63
RAN	Ranua (Finland)	65,9	26,41
LYC	Lycksele (Sweden)	64,61	18,75
OUJ	Oulujärvi (Finland)	64,52	27,23
HAN	Hankasalmi (Finland)	62,25	26,6
NUR	Nurmijärvi (Finland)	60,5	24,65
TAR	Tartu (Estonia)	58,26	26,46
BRZ	Birzai (Lithuania)	56,17	24,86
HLP	Hel (Poland)	54,61	18,82
SUW	Suwałki (Poland)	54,01	23,18
KIV	Kyiv (Ukraine)	50,81	30,27
LVV	Lviv (Ukraine)	49,9	23,75
ODE	Odesa (Ukraine)	46,78	30,9
SUA	Sulrari (Romania)	44,68	26,25

Example: digital array of 1-minute data for the Tartu Magnetic Observatory

time_min	Bx	By	Bz	B	GO_TAR
18.01.2026	15440	2961,511	49788,97	52212,12	
0,01	15441,5	2961,083	49789,25	52212,81	
0,02	15441,89	2960,74	49790,2	52213,8	
0,03	15442,49	2960,912	49790,89	52214,65	
0,04	15443,3	2960,547	49791,53	52215,48	
0,05	15443,57	2959,768	49792,44	52216,38	
0,06	15442,99	2959,317	49793,74	52217,43	
0,07	15442,02	2960,079	49795,2	52218,58	
0,08	15441,53	2961,201	49796,23	52219,48	
0,09	15442,38	2962,451	49796,85	52220,39	
0,1	15443,95	2962,75	49796,9	52220,92	
0,11	15445,51	2962,352	49797,27	52221,72	
0,12	15446,28	2962,282	49797,97	52222,61	
0,13	15446,49	2962,608	49798,77	52223,45	
0,14	15446,68	2962,535	49799,46	52224,16	
0,15	15446,94	2962,575	49800,23	52224,97	
0,16	15447,2	2963,322	49800,94	52225,77	
0,17	15447,43	2964,061	49801,47	52226,38	
0,18	15447,97	2964,958	49801,89	52226,99	

For each observatory, graphs of the northern Bx-, eastern By, vertical Bz-components and the modulus of the induction vector B were constructed.

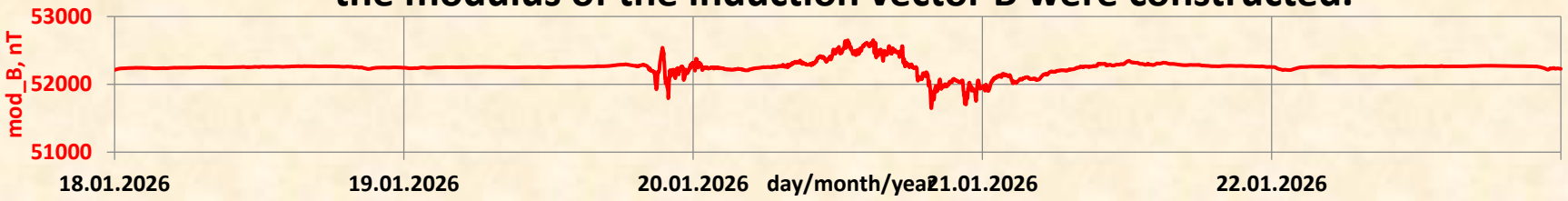

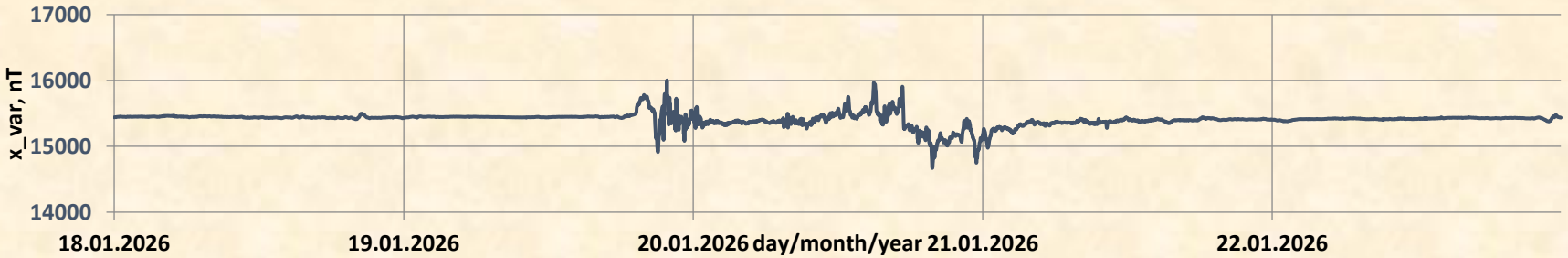

Example: Digital array of the induction vector module *B* for all Magnetic Observatory

time	KEV_B	IVA_B	SOD_B	RAN_B	LYC_B	OUJ_B	HAN_B	NUR_B	TAR_B	BRZ_B	HLP_B	SUW_B	KIV_B	LVV_B	ODE_B	SUA_B
11.11.2025	54254,97	53939,25	53308,06	53543,69	52715,1	53537,19	51891,85	52801,73	52224,54	51766,59	50853,84	51162,19	51167,61	49909,17	49986,24	48937,49
0,01	54257,33	53942,39	53310,28	53543,84	52715,2	53537,83	51892	52802,13	52224,6	51766,67	50854,24	51162,28	51167,73	49908,89	49986,4	48937,55
0,02	54259,78	53946,22	53312,92	53543,22	52714,5	53537,93	51892,41	52802,14	52224,77	51766,76	50854,4	51162,33	51167,85	49909,2	49986,48	48937,56
0,03	54260,78	53947,36	53315,04	53543,52	52715	53537,28	51892,94	52802,47	52224,86	51766,86	50854,42	51162,39	51167,84	49909,92	49986,55	48937,58
0,04	54261,62	53948,65	53316,79	53543,78	52715,8	53536,73	51893,11	52802,9	52224,93	51766,96	50854,45	51162,38	51167,94	49910,91	49986,64	48937,58
0,05	54262,08	53950,11	53317,64	53542,07	52715,5	53534,73	51892,44	52803,02	52225,04	51767,07	50854,66	51162,39	51168,05	49911	49986,87	48937,62
0,06	54261,6	53949,79	53317,23	53541,79	52714,2	53532,89	51891,3	52802,74	52225,11	51767,11	50854,92	51162,42	51168,16	49910,57	49986,93	48937,62
0,07	54262,15	53951,85	53318,07	53541,67	52712,8	53534,09	51890,79	52802,41	52225,21	51767,19	50855,16	51162,5	51168,1	49910,16	49987,09	48937,72
0,08	54262,36	53952,25	53320,23	53544,16	52711,1	53536,55	51891,22	52802,09	52225,34	51767,22	50855,39	51162,49	51168,13	49910,43	49987,09	48937,74
0,09	54261,04	53951,17	53322,6	53546,15	52710,6	53537,62	51891,57	52801,97	52225,43	51767,29	50855,36	51162,41	51168,23	49910,39	49987,25	48937,76
0,1	54260,05	53948,73	53322,9	53546,39	52712	53537,68	51891,63	52801,75	52225,58	51767,33	50855,57	51162,43	51168,3	49910,67	49987,4	48937,75
0,11	54261,77	53947,84	53323,67	53547,32	52714,7	53538,48	51892,08	52801,75	52225,76	51767,43	50855,71	51162,52	51168,46	49911,15	49987,56	48937,8
0,12	54262,07	53947,49	53326,61	53550,16	52717,2	53539,99	51892,72	52802,1	52225,92	51767,53	50855,61	51162,72	51168,39	49910,71	49987,61	48937,87
0,13	54260,87	53944,6	53329,03	53552,64	52718,4	53542,3	51893,6	52802,71	52226	51767,57	50855,63	51162,98	51168,35	49911,4	49987,59	48937,99
0,14	54261,07	53942,45	53330,08	53553,45	52719,7	53543,23	51894,7	52803,36	52225,97	51767,67	50855,41	51163,27	51168,25	49912,16	49987,5	48938,15
0,15	54262,11	53940,37	53329,97	53553,04	52721,5	53541,9	51894,87	52804,12	52225,84	51767,68	50855,18	51163,44	51168,2	49911,91	49987,38	48938,27
0,16	54267,91	53943,73	53328,27	53553,23	52721,5	53540,88	51894,4	52804,24	52225,7	51767,68	50855,12	51163,49	51168,2	49911,68	49987,32	48938,33
0,17	54273,6	53946,53	53327,18	53553,74	52720,7	53540,74	51893,66	52804,25	52225,73	51767,71	50855,05	51163,47	51168,32	49911,58	49987,42	48938,37
0,18	54277,74	53947,13	53325,29	53553,64	52718,6	53542,29	51893,48	52804,16	52225,75	51767,71	50855,21	51163,52	51168,27	49911,46	49987,36	48938,39

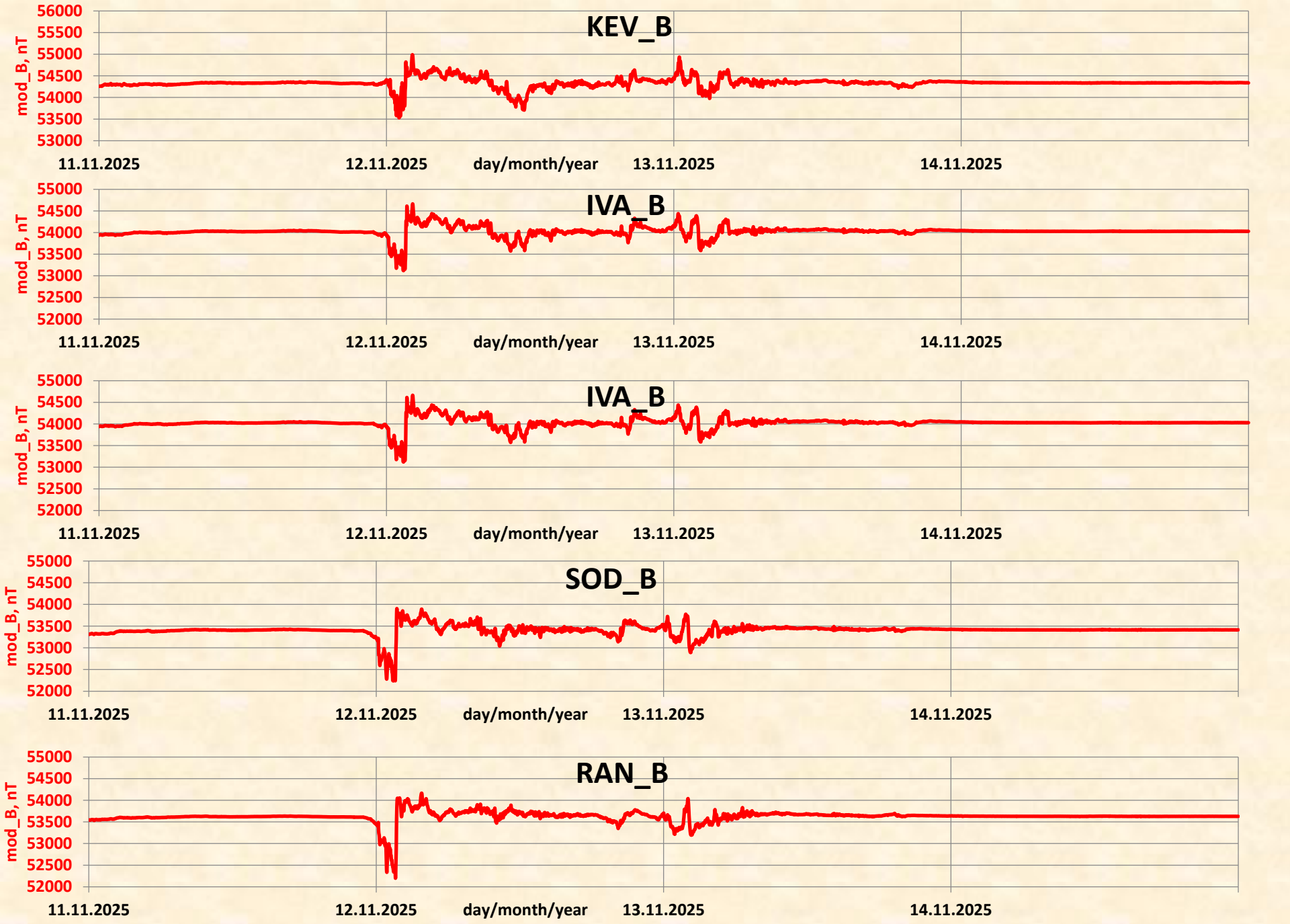
KEV_B
mod_B, nT
56000
55500
55000
54500
54000
53500
53000
11.11.2025
12.11.2025
day/month/year
13.11.2025
14.11.2025
IVA_B
mod_B, nT
55000
54500
54000
53500
53000
52500
52000
11.11.2025
12.11.2025
day/month/year
13.11.2025
14.11.2025
IVA_B
mod_B, nT
55000
54500
54000
53500
53000
52500
52000
11.11.2025
12.11.2025
day/month/year
13.11.2025
14.11.2025
SOD_B
mod_B, nT
55000
54500
54000
53500
53000
52500
52000
11.11.2025
12.11.2025
day/month/year
13.11.2025
14.11.2025
RAN_B
mod_B, nT
55000
54500
54000
53500
53000
52500
52000
11.11.2025
12.11.2025
day/month/year
13.11.2025
14.11.2025

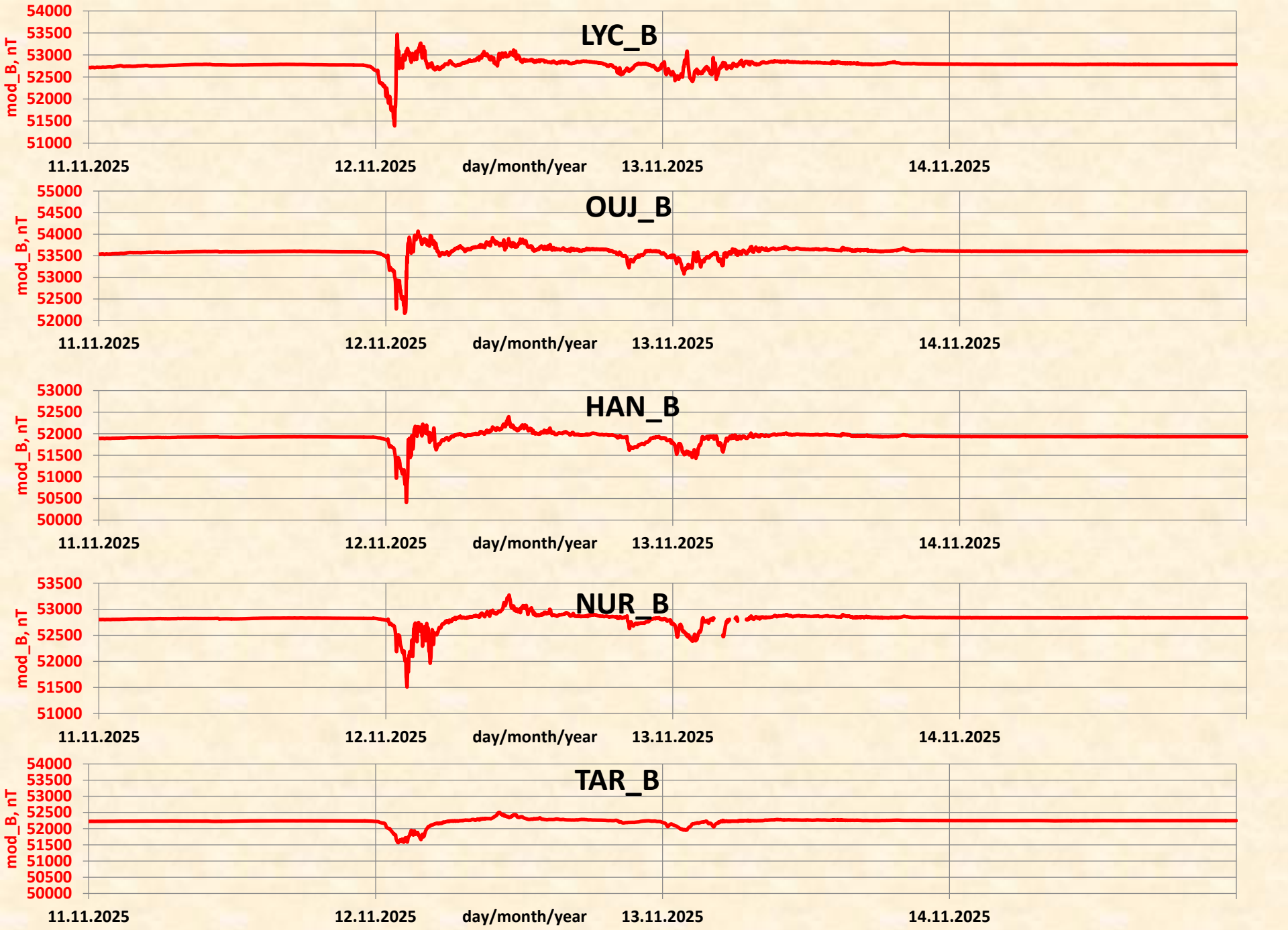
LYC_B
mod_B, nT
54000
53500
53000
52500
52000
51500
51000
11.11.2025
12.11.2025
day/month/year
13.11.2025
14.11.2025
OUJ_B
mod_B, nT
55000
54500
54000
53500
53000
52500
52000
11.11.2025
12.11.2025
day/month/year
13.11.2025
14.11.2025
HAN_B
mod_B, nT
53000
52500
52000
51500
51000
50500
50000
11.11.2025
12.11.2025
day/month/year
13.11.2025
14.11.2025
NUR_B
mod_B, nT
53500
53000
52500
52000
51500
51000
11.11.2025
12.11.2025
day/month/year
13.11.2025
14.11.2025
TAR_B
mod_B, nT
54000
53500
53000
52500
52000
51500
51000
50500
50000
11.11.2025
12.11.2025
day/month/year
13.11.2025
14.11.2025

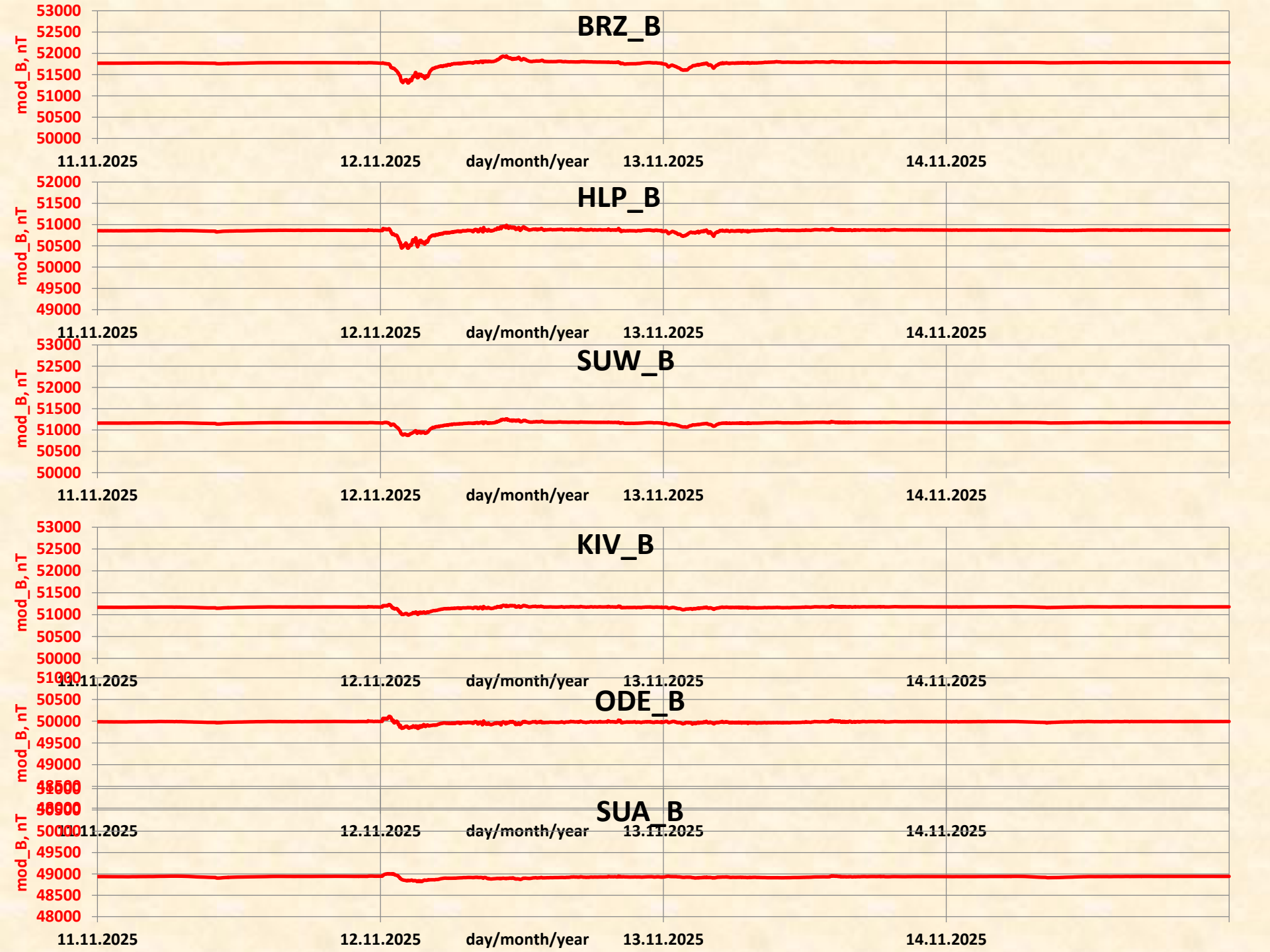
BRZ_B
HLP_B
SUW_B
KIV_B
ODE_B
SUA_B
mod_B, nT
11.11.2025
12.11.2025
day/month/year
13.11.2025
14.11.2025

Parameters of the induction vector module B and its magnetic storm component 18-22.01.2026 for all observatories

Kod	Name (country)	Latitude	Longitude	x_min	y_min	z_min	B_min	x_max	y_max	z_max	B_max	δBx (max-min)	δBy (max-min)	δBz (max-min)	δB (max-min)	δB_aver	Bn_01_2026
KEV	Kevo (Finland)	69,76	27,01	9109,8	2322,0	52522,6	53608,4	10705,5	3645,9	54135,9	55051,1	1595,74	1323,88	1613,29	1442,71	54322,25	54444
IVA	Ivalo (Finland)	68,56	27,29	9321,3	2565,5	52194,9	53231,8	10996,3	3839,6	53660,1	54634,7	1675,00	1274,13	1465,16	1402,88	53998,09	54272
SOD	Sodankylä (Finland)	67,37	26,63	9821,0	2215,9	51439,2	52577,6	11568,4	3405,8	53026,4	54022,5	1747,40	1189,90	1587,20	1444,84	53367,51	54020
RAN	Ranua (Finland)	65,9	26,41	8979,8	3426,5	51715,2	52836,1	11188,9	4615,1	53035,3	54040,5	2209,08	1188,61	1320,06	1204,38	53576,20	53749
LYC	Lycksele (Sweden)	64,61	18,75	11042,8	1447,2	50483,2	51992,5	13611,2	2687,9	51885,4	53218,9	2568,40	1240,70	1402,20	1226,40	52729,11	52939
OUJ	Oulujärvi (Finland)	64,52	27,23	10901,4	2359,9	51182,0	52702,7	13199,6	3722,9	52505,4	53926,1	2298,23	1363,04	1323,39	1223,34	53547,61	53579
HAN	Hankasalmi (Finland)	62,25	26,6	11570,5	2441,9	49354,2	51025,9	13441,2	3858,9	50515,4	52268,2	1870,68	1417,01	1161,23	1242,30	51900,46	53111
NUR	Nurmijärvi (Finland)	60,5	24,65	13950,2	2099,7	50136,1	52187,1	15063,3	2848,0	50923,5	53076,5	1113,12	748,33	787,36	889,37	52821,71	52606
TAR	Tartu (Estonia)	58,26	26,46	14670,1	2759,7	49277,9	51647,3	16001,6	3305,5	50185,1	52651,8	1331,51	545,85	907,27	1004,47	52236,92	52330
BRZ	Birzai (Lithuania)	56,17	24,86	15862,2	2510,8	48747,3	51396,5	17054,7	3031,7	49419,7	52220,3	1192,54	520,85	672,43	823,82	51781,86	51753
HLP	Hel (Poland)	54,61	18,82	16931,4	1764,1	47506,5	50582,0	17796,0	2365,8	48202,8	51355,8	864,59	601,72	696,29	773,78	50873,41	50920
SUW	Suwałki (Poland)	54,01	23,18	17171,8	2272,4	47896,2	50966,3	17761,0	2711,2	48464,6	51613,9	589,21	438,79	568,46	647,63	51179,42	51136
KIV	Kyiv (Ukraine)	50,81	30,27	18841,1	2837,4	47327,5	51058,5	19355,2	3271,3	47581,7	51293,4	514,10	433,90	254,20	234,83	51166,75	51071
LVV	Lviv (Ukraine)	49,9	23,75	19585,6	2158,0	45697,6	49792,8	20106,5	2564,2	45986,4	50070,7	520,90	406,20	288,80	277,85	49917,60	50211
ODE	Odesa (Ukraine)	46,78	30,9	20851,09	1967,71	45240,3	49814,06	21440,06	2350,86	45444,3	50094,61	588,97	383,15	204,00	280,55	49981,83	50084
SUA	Sulrari (Romania)	44,68	26,25	22278,0	2425,7	43331,0	48854,9	22860,2	2753,7	43464,6	49057,1	582,20	327,99	133,60	202,15	48929,21	49007

GENERAL CHARACTERISTICS OF THE GEOMAGNETIC STORM 18-22.01.2026

Bmax-Bmin

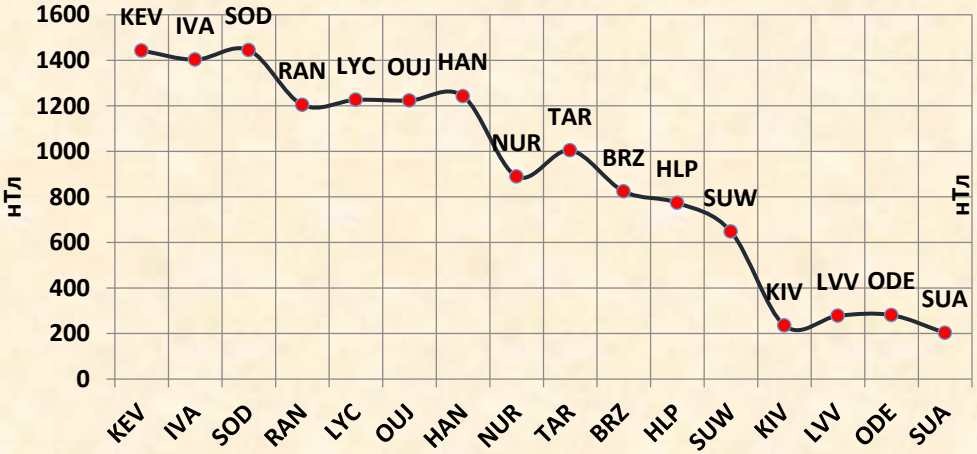

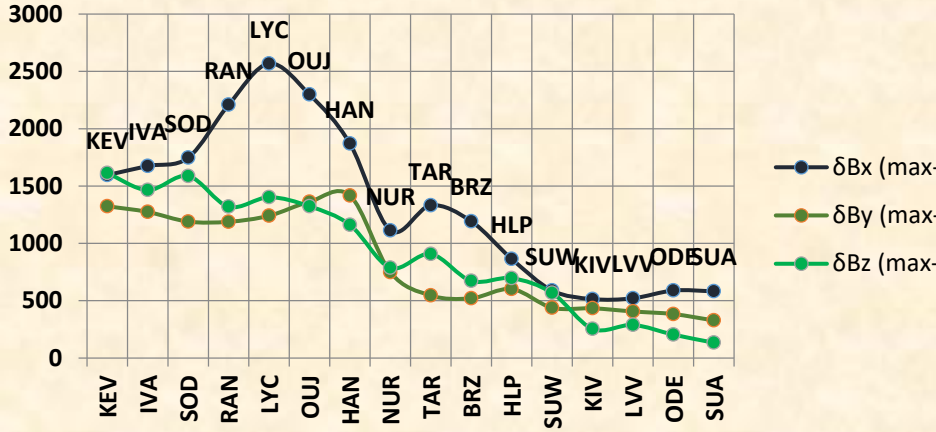

δB_aver

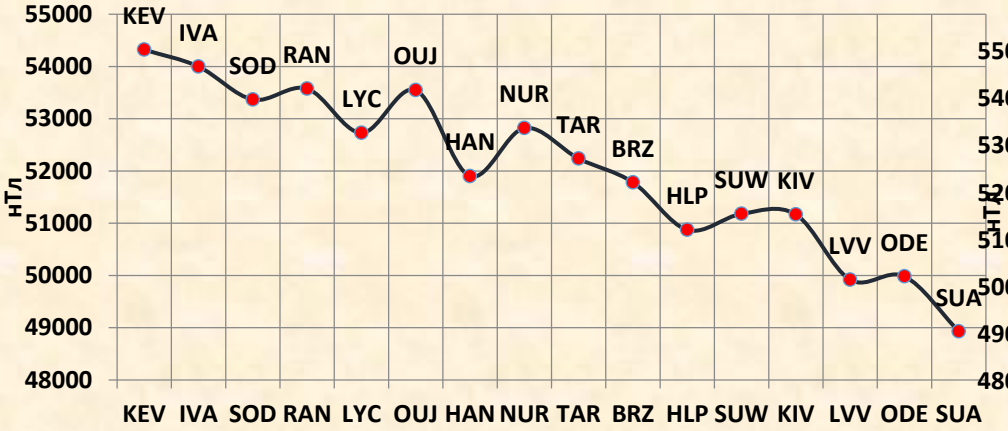

Bn_01_2026

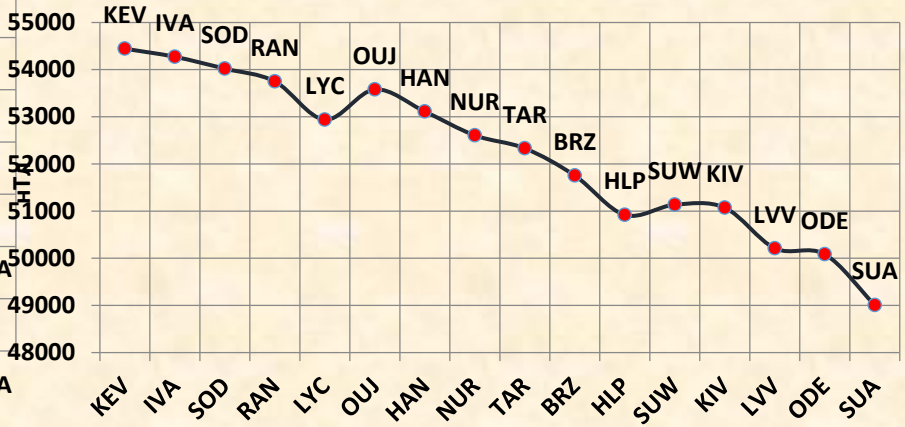

Parameters of the induction vector module B and its magnetic storm component 11-14.11.2025 for all observatories

Kod	Name (country)	Latitude	Longitude	x_min	y_min	z_min	B_min	x_max	y_max	z_max	B_max	δBx (max-min)	δBy (max-min)	δBz (max-min)	δB (max-min)	δB_aver	Bn_11_2025
KEV	Kevo (Finland)	69,76	27,01	8029,331	1783,431	52548,45	53527,84	10943,65	3850,715	53987,89	54987,08	2914,322	2067,2845	1439,439	1459,23	54342,08	54434
IVA	Ivalo (Finland)	68,56	27,29	7917,447	2117,35	52274,81	53120,32	11308,43	3816,855	53639,51	54662,98	3390,981	1699,50567	1364,695	1542,66	54026,81	54262
SOD	Sodankylä (Finland)	67,37	26,63	8692,9	1480,3	51311,8	52240,94	11789,1	3180,5	52890,1	53903,33	3096,2	1700,2	1578,3	1662,39	53403,84	54010
RAN	Ranua (Finland)	65,9	26,41	8644,67	3065,664	51302,56	52197,97	11282,54	4468,083	53056,6	54163,59	2637,866	1402,41933	1754,034	1965,61	53623,01	53740
LYC	Lycksele (Sweden)	64,61	18,75	10169,2	1006,2	50123,1	51389	13501,9	2586,4	52052,4	53471,5	3332,7	1580,2	1929,3	2082,50	52776,12	52931
OUJ	Oulujärvi (Finland)	64,52	27,23	9782,262	2389,069	50909,88	52164,96	13256	3565,401	52546,9	54069,06	3473,739	1176,33167	1637,018	1904,10	53585,73	53569
HAN	Hankasalmi (Finland)	62,25	26,6	11064,29	2655,111	48985,61	50406,22	13403,92	3948,242	50644,52	52395,23	2339,631	1293,1315	1658,915	1989,01	51907,6	53101
NUR	Nurmijärvi (Finland)	60,5	24,65	13227,36	2137,98	49655,96	51506,84	15003,12	2853,38	51065,67	53272,3	1775,76	715,4	1409,71	1765,46	52783,48	52596
TAR	Tartu (Estonia)	58,26	26,46	14736,68	2635,17	49286,97	51567,46	15627,13	3156,361	50063,92	52503,15	890,453	521,190833	776,95	935,68	52197,96	52320
BRZ	Birzai (Lithuania)	56,17	24,86	16025,93	2347,634	48647,9	51302,24	16635,57	2830,386	49195,41	51936,94	609,6415	482,752	547,5138	634,70	51746,44	51742
HLP	Hel (Poland)	54,61	18,82	17040,71	1683,75	47394,61	50445,93	17681,88	2119,87	47887,69	50983,36	641,17	436,12	493,08	537,43	50833,46	50910
SUW	Suwałki (Poland)	54,01	23,18	17180,18	2170,101	47797,12	50874	17705,76	2554,022	48160,67	51259,14	525,572	383,920167	363,5533	385,14	51144,89	51126
KIV	Kyiv (Ukraine)	50,81	30,27	18836	2694,7	47264,4	50995,09	19278,6	3064,2	47477,3	51230,03	442,6	369,5	212,9	234,94	51153,57	51060
LVV	Lviv (Ukraine)	49,9	23,75	19574,9	2064,8	45608,5	49727,49	20038,3	2397,3	45832,9	49977,09	463,4	332,5	224,4	249,60	49893,27	50201
ODE	Odesa (Ukraine)	46,78	30,9	20930,95	1852,66	45182,8	49835,45	21375,06	2170,16	45365,3	50112,48	444,11	317,5	182,5	277,03	49965,24	50073
SUA	Sulrari (Romania)	44,68	26,25	22367,68	2339,18	43303,2	48820,64	22805,5	2610,18	43401,6	49006,26	437,82	271	98,4	185,62	48913,8	48997

GENERAL CHARACTERISTICS OF THE GEOMAGNETIC STORM 11-14.11.2025

Bmax-Bmin

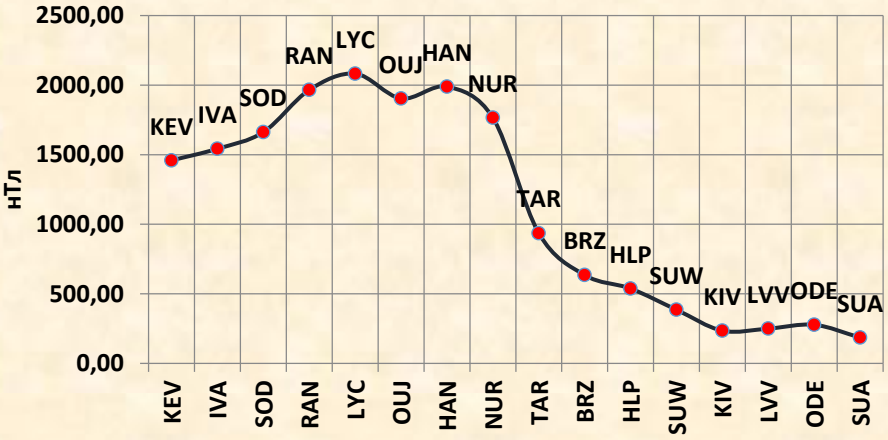

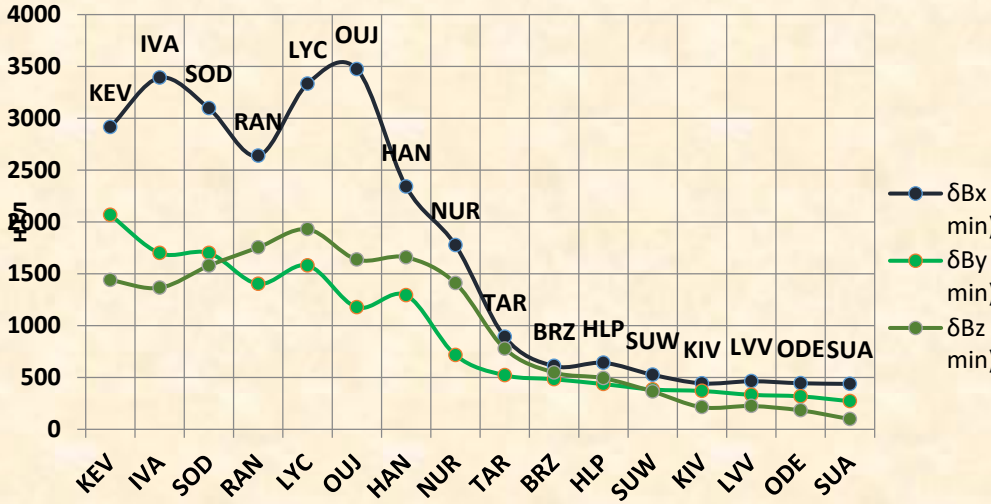

δB_aver

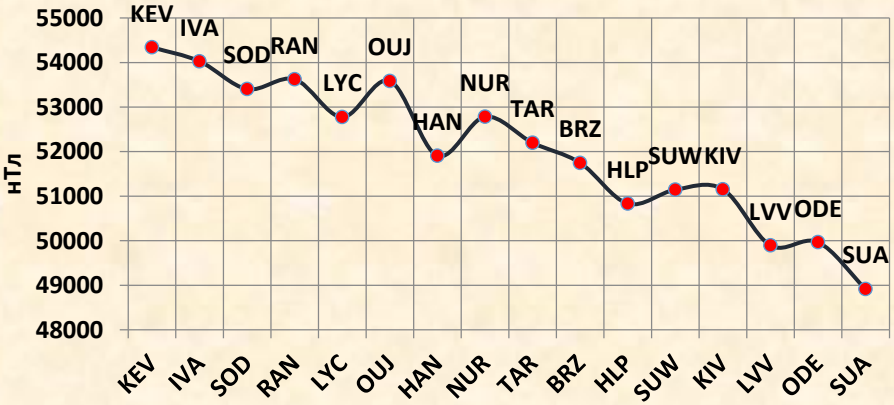

Bn_11_2025

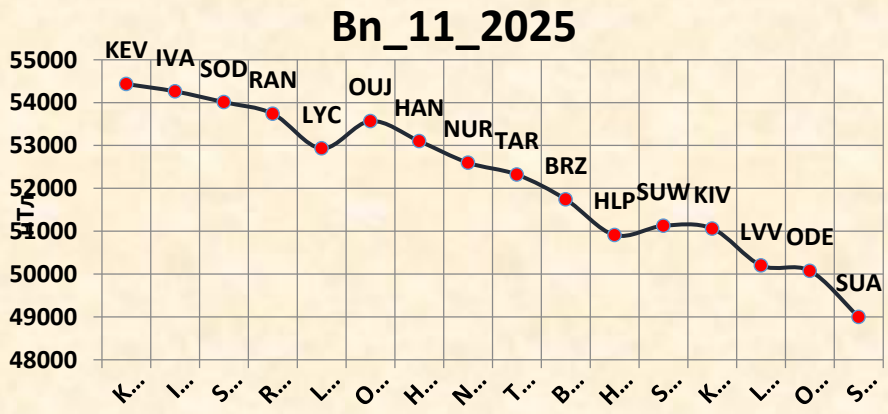

The magnetic field of the Earth's lithosphere in the “Struve Arc” region for the Epoch 2025

At the altitude of 4 km)

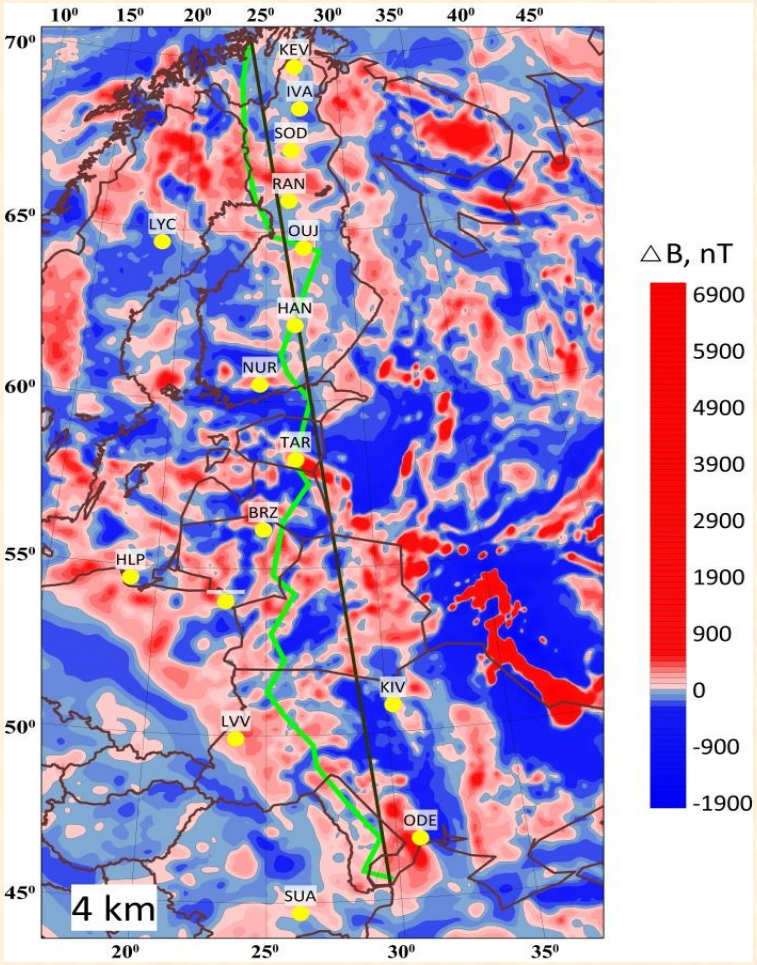

At an altitude of 100 km

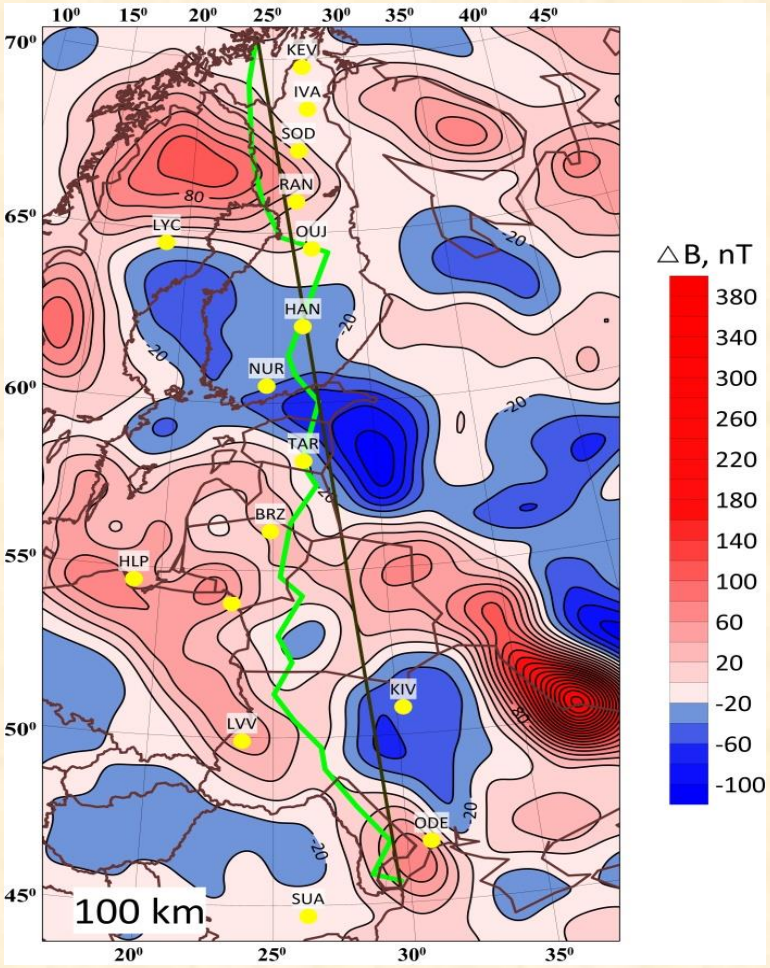

At the altitude of 4 km the magnetic field of the Earth's lithosphere varies within ±(400÷800) nT and at an altitude of 100 km - ±(60÷100) nT. Anomalous zones are caused by the superposition of regional anomalies. In the zones of positive anomalies, there are SOD, RAN, OUJ, HLP, BRZ, SUV, LVV, ODE observatories, and in the negative ones - NUR, SUR.

At the altitude of 150 km the magnetic field of the Earth's lithosphere varies within ±(80÷220) nT and at an altitude of 200 km - ±(60÷140) nT.

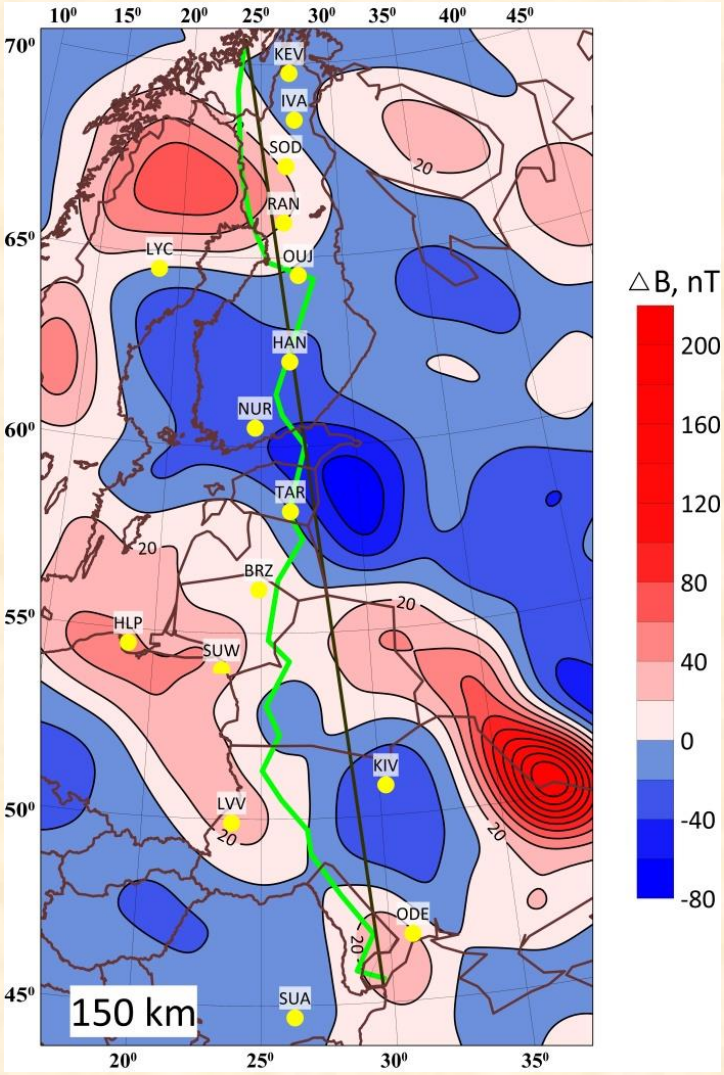

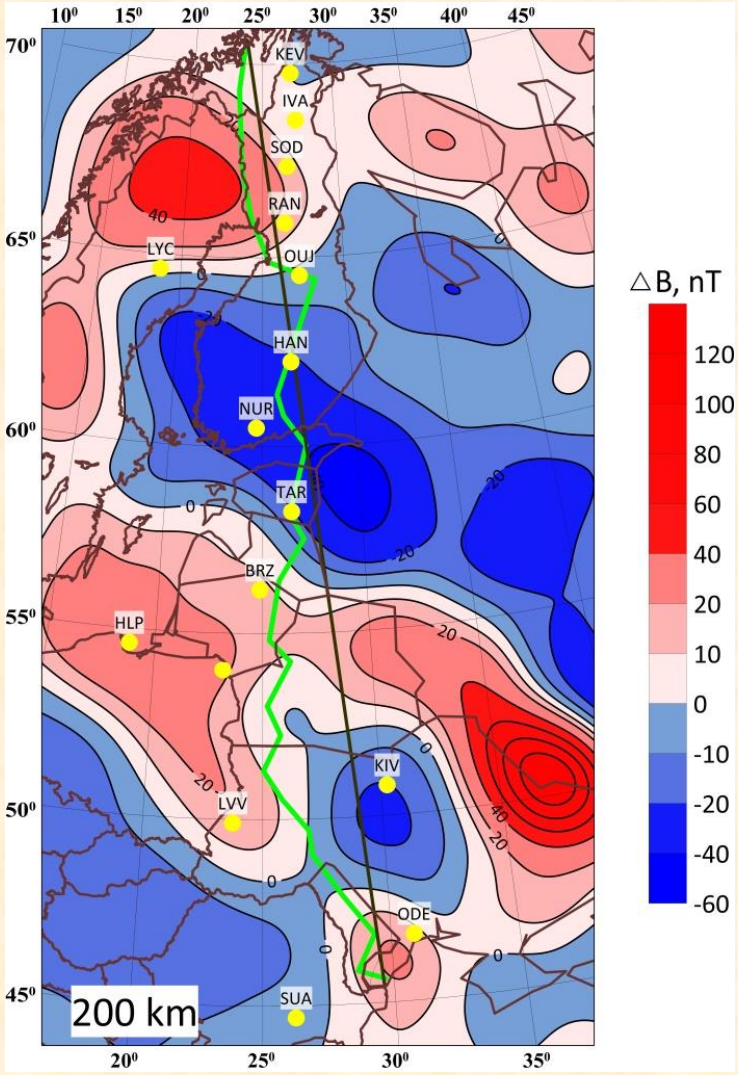

At the altitude of 250 km the magnetic field of the Earth's lithosphere varies within ±(40÷85) nT and at an altitude of 300 km - ±(40÷55) nT.

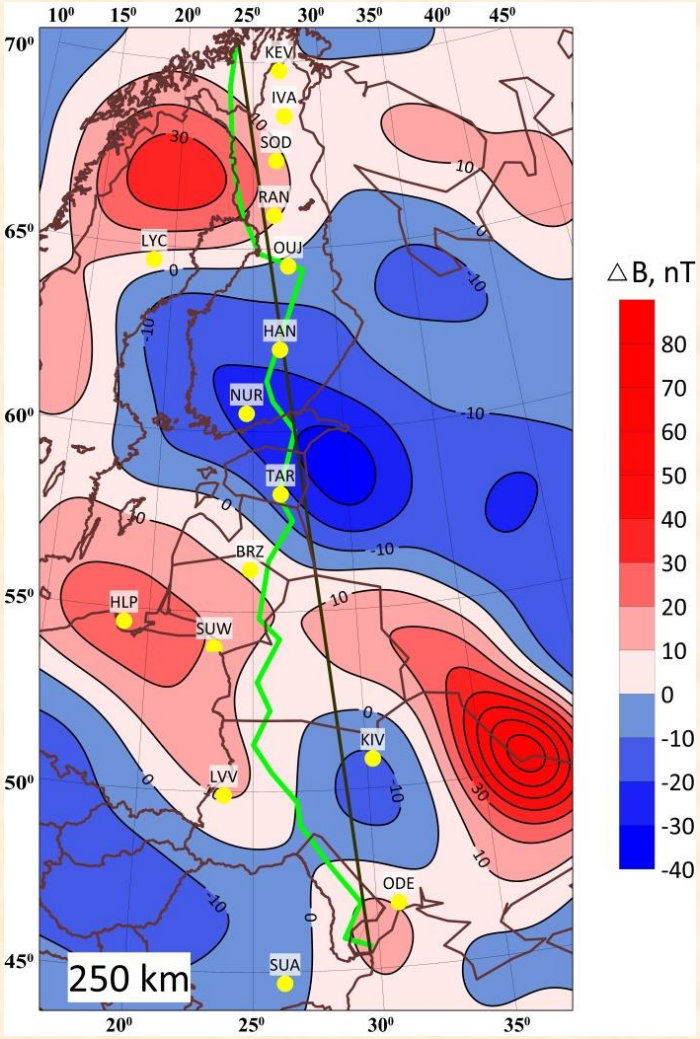

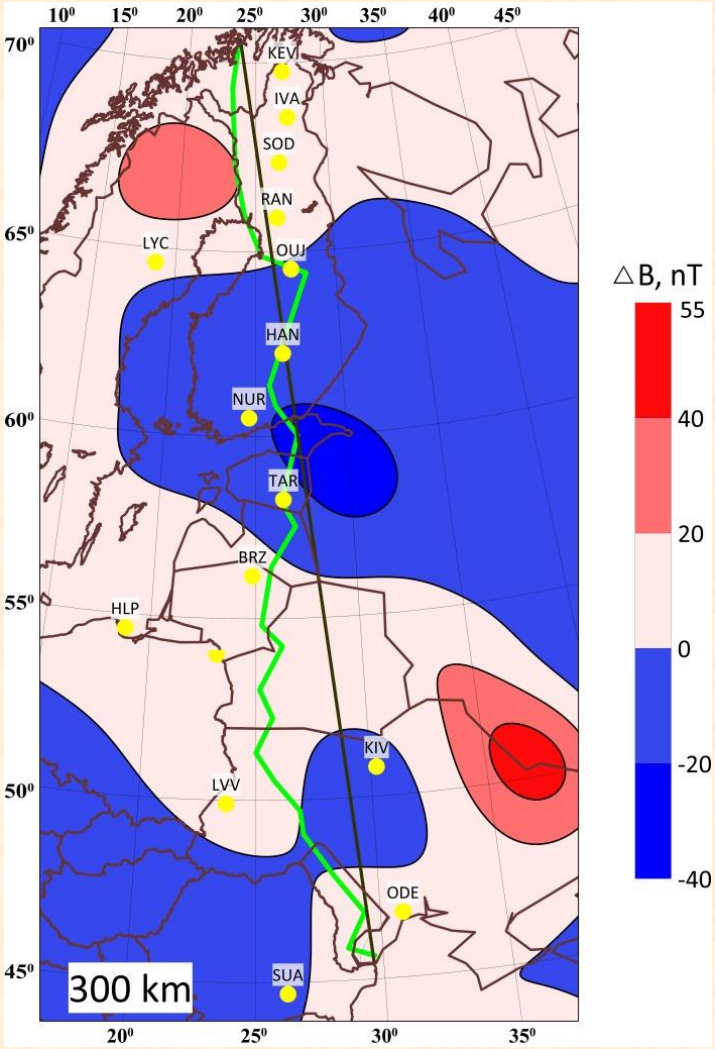

SUMMARY

Initial digital data from 17 magnetic stations along the "Struve Geodetic Arc" meridian for magnetic storms on 11-14.11.2025 and 18-22.01.2025 have been accumulated. Preliminary calculations of the geomagnetic field induction modulus and its variations have been performed for the purpose of their further analysis. Maps of the anomalous magnetic field on the Earth's surface and ionospheric heights with magnetic station points have been presented. The obtained data will be the basic elements of the "geomagnetic part" of space weather monitoring.

Thank you for attention!
SLAVA UKRAINI!!!